

## **Elemental distribution in zircon: Alteration and radiation-damage effects**

KENJI HORIE<sup>1\*</sup>, HIROSHI HIDAKA<sup>1,2</sup> AND FRANÇOIS GAUTHIER-LAFAYE<sup>3</sup>

<sup>1</sup>Department of Earth and Planetary Systems Science, Hiroshima University  
Higashi-Hiroshima 739-8526, Japan

<sup>2</sup>Project Center of Multi-Isotope Research for Astro- & Geochemical Evolution  
(MIRAGE)

Hiroshima University, Higashi-Hiroshima 739-8526, Japan

<sup>3</sup>Ecole et Observatoire des Sciences de la Terre, UMR7517-CNRS-ULP  
1 rue Blessig, 67084 Strasbourg, France

\*Author to whom correspondence should be addressed ([kenjih@hiroshima-u.ac.jp](mailto:kenjih@hiroshima-u.ac.jp))

## Abstract

Isotopic analyses of U, Pb and REE in 144 zircon grains from the Bidoudouma stream, the Republic of Gabon, were performed to study correlation of elemental distribution with geological alteration effects. The U-Pb isotopic results reveal that the zircons formed around 2.8-2.1 Ga ago and altered around 500 Ma ago by igneous activity in association with dolerite dyke intrusion. The REE abundance patterns of the U-Pb discordant zircons are characterized by high contents of REE (977-98154 ppm), small LREE-HREE fractionations and distinctly positive Eu anomalies. The discordant zircons also contain significant amounts of non-formula elements such as Ca, Mn, Al and Fe; whereas, their contents of Zr and Si are 1-15% lower than those of concordant zircon. Non-formula elements and REE, especially LREE, were incorporated into metamict zircon in association with Pb-loss, which indicates that the non-formula elements and REE substituted for Zr and Si. Judging from this correlation among the contents of non-formula elements, when zircon was initially altered, Fe substituted for major elements of zircon. After the saturation of Fe, Ca and Mn were incorporated into zircon together with REE and Al followed by Ca. The metamict zircons contain large amount of U (~8215 ppm), which indicates that U had not migrated from zircon grain in association with the Pb-loss.

## Keywords

metamict zircon / alteration / incorporation / REE / U-Pb systematics / Bidoudouma

## 1. INTRODUCTION

Zircon is one of accessory minerals which are suited for *in-situ* U-Pb geochronology and has been proposed as an immobilization phase for actinides because of the ability to incorporate large amounts of U and Pu (e.g., Ewing et al., 1995; Ewing, 1999). In these applications, the redistribution and/or retention behavior of trace elements such as Pb, U and rare earth elements (REE) is important and elemental release may be much enhanced by radiation damage caused by the  $\alpha$ -decay of constituent actinides (Ewing et al., 1988, 2003). Previous work reports incorporation of light REE (LREE) and non-formula elements such as Ca, Al, Fe and Mn into metamict zircon in association with hydrothermal alteration (e.g., Geisler et al., 2002, 2003). Geisler et al. (2002) suggested loss of U and Th from zircon during low temperature leaching experiments, whereas Mathieu et al. (2001) concluded that U enriched rim of zircon was caused by an incorporation of U together with LREE. In this paper, we investigate the distribution of U, REE and non-formula elements in metamict zircon in association with the disturbance of U-Pb system using *in-situ* isotopic analysis via an ion microprobe.

## 2. EXPERIMENTAL PROCEDURES

### 2.1. Samples

The samples used in this study were collected from the Bidoudouma stream which is located 63km north of Oklo, the Republic of Gabon (Fig.1). The rocks consist of fine-grained (0.1 to 0.2 mm) acidic tuff, and contain quartz and albite grains. The matrix is dominated by quartz and feldspar with small amount of chlorite and epidote. Muscovite, biotite, zircon, apatite, tourmaline and garnet occur as accessory minerals. The occurrence of non-volcanic minerals such as muscovite, tourmaline and garnet reflects the origin of the detrital minerals. Some samples include small veins of

Fe-bearing minerals and contain some altered monazite.

## 2.2. Analytical Procedures

An electron probe micro analyzer (EPMA: JEOL JXA-8200) was used for quantitative analysis of major elements and for obtaining back-scattered electron (BSE) images of individual zircon grains. The analytical spot size was 5  $\mu\text{m}$ , and the electron beam current was 50 nA at 15 kV of acceleration voltage. *In-situ* isotopic analyses of Pb, U and REE were performed on a Sensitive High-mass Resolution Ion MicroProbe (SHRIMP II) at Hiroshima University. A 0.5-1.2 nA beam of  $\text{O}_2^-$  primary ion was used to sputter a 10  $\mu\text{m}$  analytical spot on the sample. Prior to SHRIMP measurements, analytical spots were selected by using a BSE image and reflected light microscopy to avoid micro fractures and inclusions in the individual zircon grains. The procedures for Pb and U isotopic analyses of zircon are after Compston et al. (1984). In this study, two kinds of standard zircon, QGNG ( $^{206}\text{Pb}/^{238}\text{U}=0.3307$ ;  $1842.0\pm 3.1$  Ma (Black et al., 2004)) and SL13 (U concentration of 238 ppm) were used for the U-Pb calibration and the calculation of U and REE concentrations in the samples, respectively. The determination of REE abundances of zircon was based on the analytical procedures of Hidaka et al. (2002). Raman spectroscopy was completed on a Renishaw inVia Raman Reflex microscope with a dedicated Leica DMLM microscope using 100x objective lens at Hiroshima University. Spectra were excited with the 514 nm emission line of an Ar laser (20 mW). The scattered Raman light was analyzed with a charge-coupled device (CCD) array detector after being dispersed by a grating at 1800 grooves per mm. Detailed analytical procedures are after Nasdala et al. (1995).

## 3. RESULTS AND DISCUSSION

### 3.1. U-Pb system

Overall 144 zircon grains were identified in three thin sections and the grain

size is variable from less than 10 to 200  $\mu\text{m}$ . Over 130 zircon grains show distinct discordant U-Pb data (Fig. 2a), suggesting disturbance of the U-Pb system in the individual grains. U-Pb data of the discordant zircons show 2.8-2.1 Ga as an upper intercept age of the U-Pb concordia diagram in Fig. 2a, which is consistent with previous chronological data for the Bidoudouma stream (Horie et al., 2004). U contents of discordant zircon (100-8215 ppm) are higher than those of concordant zircon (30-581 ppm). High U content is possibly due to variable radiation damage to crystal structure, resulting in the metamict state. The low crystallinity zircons are more susceptible to alteration and easily release Pb from the structure (e.g., Pidgeon et al., 1966). In order to quantify the degree of radiation damage of discordant zircons, micro-Raman spectroscopy was used. As shown in Fig. 2b, the full width at half maximum (FWHM) of the intense  $\nu_3(\text{SiO}_4)$  stretching band around  $1000\text{ cm}^{-1}$  increases with time-integrated self-irradiation doses ( $D_\alpha$ ) calculated from the measured U and Th concentrations using the upper intercept ages of each of the zircon grains. Phonon frequencies of  $\nu_3(\text{SiO}_4)$  band also increase with  $D_\alpha$ . The effects of  $\alpha$ -decay radiation damage on zircon structure are characterized by a decrease in Raman intensity, an increase of FWHM and a decrease in phonon frequencies of  $\nu_3(\text{SiO}_4)$  (e.g., Zhang et al., 2000; Nasdala et al., 2003; Palenik et al., 2003). Moreover, as shown in Fig. 2c, zircon grains with high  $D_\alpha$  lost Pb and major constituent elements such as Zr and Si. These correlations between  $D_\alpha$  and a degree of Pb-loss indicate that the metamict zircons have released Pb through low crystallinity or amorphous phase in association with geological events (Utsunomiya et al., 2004). The decrease of major elements suggests replacement of other elements such as REE and non-formula elements in association with Pb-loss (Geisler et al., 2003).

### **3.2. Incorporation of REE and non-formula elements into metamict zircon**

Figure 3a shows typical REE patterns normalized by C1 chondrite of the

Bidoudouma zircons. Discordant zircons show larger amounts of total REE ( $\Sigma\text{REE}=977\text{-}98154$  ppm) and less fractionation between LREE (La, Pr and Nd) and HREE (Tm, Yb and Lu) ( $\text{HREE/LREE}=1.9\text{-}208$ ) rather than concordant zircons ( $\Sigma\text{REE}=383\text{-}801$  ppm;  $\text{HREE/LREE}=129\text{-}2166$ ). Some of the discordant zircon show distinctly positive Eu anomalies ( $\text{Eu/Eu}^*=0.47\text{-}4.5$ ;  $\text{Eu}^*$  is defined as  $(\text{Sm}+\text{Gd})/2$  in chondrite-normalized REE patterns) which is not common in the terrestrial minerals. There are two reasons suggested for the difference in REE data between concordant and discordant zircon grains; (1) the REE abundances in the discordant zircon may reflect the original chemical compositions of the source melt rock. (2) the REE were redistributed in zircon during the thermal event in association with dolerite dyke intrusion (Evins et al., 2005). Considering the chemical similarity between REE and U, it seems reasonable that discordant zircons with higher U contents contain larger amounts of REE. As shown in Fig. 3a, the Eu change from deficit to excess to a reference value  $\text{Eu}^*$  within a single grain, and it is unlikely that melts with different chemical composition existed contemporaneously within such a narrow composition range. Previous work reported preferential incorporation of LREE into metamict zircon together with non-formula elements in association with depletion of Zr and Si contents (e.g., Mathieu et al., 2001; Geisler et al., 2003). The discordant zircons of the Bidoudouma contain large amounts of Ca (CaO: 0-1.65 wt.%), Mn (MnO: 0-0.66 wt.%), Al ( $\text{Al}_2\text{O}_3$ : 0-1.85 wt.%) and Fe (FeO: 0.04-0.93 wt.%) as compared with concordant zircon (CaO, Mn and  $\text{Al}_2\text{O}_3$ : <0.01 wt.%; FeO: <0.15 wt.%). On the other hand, Zr and Si contents of discordant zircon ( $\text{ZrO}_2$ : 55.5-65.4 and  $\text{SiO}_2$ : 30.6-34.0 wt.%) are lower than those of concordant zircon ( $\text{ZrO}_2$ : 64.4-66.0 and  $\text{SiO}_2$ : 33.2-34.2 wt.%). Figure 3b shows a correlation between the contents of Zr and Ca, and the other non-formula elements such as Mn, Al and Fe also show the correlation with those of Zr and Si. These correlations suggest that non-formula elements substituted for Zr and Si.

Judging from the correlation between Zr contents and the degree of Pb-loss (Fig. 2c), the incorporation of non-formula elements was associated with Pb-loss. Considering the similarity of the ionic radii among  $\text{Ca}^{2+}$  (1.12 Å),  $\text{Mn}^{2+}$  (0.96 Å) and  $\text{REE}^{3+}$  (La and Lu: 1.16 and 0.977 Å, respectively), there is a possibility that the REE incorporated into the metamict zircon in association with the substitution of Ca and Mn. As shown in Fig. 3b, the discordant zircons show higher concentrations of Ca than those of Mn, which indicates preferential incorporation of LREE into metamict zircons rather than HREE. Therefore, small LREE-HREE fractionations ( $\text{HREE/LREE} < 208$ ) in discordant zircons result from the preferential incorporation of LREE together with Ca.

Some zircons with high Zr-content have no correlation between contents of Zr and Ca (Fig. 3b). In the high Zr region,  $\text{ZrO}_2$  contents decrease from 66 to ca. 64 wt.%; whereas, Ca and Mn contents are constant ( $\text{CaO} < 0.01$  and  $\text{MnO} < 0.03$  wt.%, respectively). On the other hand, FeO contents increase from 0.03 to 0.3 wt.% in the same high Zr region. Figure 3c shows a correlation between Ca content and Fe and Al contents. Fe-content rapidly increases in low Ca region ( $\text{CaO} < 0.08$  wt.%), and was kept constant at  $\text{CaO} > 0.08$  wt.%. The correlation between the contents of Ca and Fe seems to be logarithmic, which suggests that Fe contents are saturated above 0.08 wt.% of CaO. The region of the rapid increase of Fe-content accords with the region of the decrease of Zr-content without enrichment of Ca, which indicates that the decrease of Zr-content before the enrichment of Ca was caused by incorporation of Fe. On the other hand, Al contents of discordant zircon are constant below 0.5 wt.% of CaO and exponentially increase above 0.5 wt.%. The experimental results of hydrothermal treatment of natural zircons (Geisler et al., 2001) also support this correlation. Moreover, our data suggest the substitution mechanism of non-formula elements into altered zircon. When zircon was initially altered, Fe substituted for major elements of

zircon. After the saturation of Fe (around 0.5 wt.%), Ca and Mn incorporated into zircon together with REE and Al followed Ca.

### **3.3. Redistribution behavior of U**

As shown in Fig. 4, zircons with high U content lost large amounts of Pb. High U content in zircon caused radiation damage to the crystal structure, and metamict zircon easily released Pb. The correlation between U contents and the degree of Pb-loss indicates that Pb-loss easily occurred in highly metamict zircons. Geisler et al. (2002) found over 90 % of U migrated from zircon in association with Pb-loss of ca. 98 % through hydrothermal alteration; whereas, Mathieu et al. (2001) reported an enrichment of U in detrital zircons around uranium deposit. The metamict zircons released over 80 % of Pb maintain large amounts of U (1000~2300 ppm), which suggests that mobility of U in association with the Pb-loss was not high.

## **4. CONCLUSIONS**

Many zircon grains of the Bidoudouma show distinctly discordant U-Pb data. Raman spectra indicated that crystal structure of the discordant zircons was damaged by  $\alpha$ -decay radiation. The REE abundance patterns of the discordant zircons are characterized by large amount of REE, small LREE-HREE fractionations and distinctly positive Eu anomalies. The discordant zircons contain large amount of Ca, Mn, Al and Fe; whereas, Zr and Si contents of discordant zircon are 1-15% lower than those of concordant zircon. These non-formula elements substituted for Zr and Si in association with Pb-loss. Considering the similarity of the ionic radii among  $\text{Ca}^{2+}$ ,  $\text{Mn}^{2+}$  and  $\text{REE}^{3+}$ , REE incorporated into metamict zircon in association with the incorporation of Ca and Mn. Judging from this correlation among the contents of non-formula elements, when zircon was initially altered, Fe substituted for major elements of zircon. After the saturation of Fe, Ca and Mn incorporated into zircon



together with REE and Al followed Ca. The metamict zircons contain large amounts of U (~8215 ppm), which suggests that U had not migrated from the zircon grains in association with the Pb-loss.

#### *Acknowledgements*

Thanks are expressed to Y. Shibata and Y. Hayasaka for their technical help with EPMA analyses. This study was financially supported by a doctoral fellowship grant (to K.H., No.05203) and a Grant-in-Aid for Scientific Research (to H.H., No. 17204051) from the Japan Society for the Promotion of Science (JSPS). This is an EOST/CGS contribution no. 2005.201-UMR7517.

## REFERENCES

- Black, L.P., Kamo, S.L., Allen, C.M., Davis, D.W., Aleinikoff, J.N., Valley, J.W., Mundil, R., Campbell, I.H., Korsch, R.J., Williams, I.S., Foudoulis, C., 2004. Improved  $^{206}\text{Pb}/^{238}\text{U}$  microprobe geochronology by the monitoring of a trace-element-related matrix effect; SHRIMP, ID-TIMS, ELA-ICP-MS and oxygen isotope documentation for a series of zircon standards. *Chem. Geol.* 205, 115-140.
- Compston, W., Williams, I.S., Meyer, C.E., 1984. U-Pb geochronology of zircons from lunar breccia 73217 using a sensitive high-mass resolution ion microprobe. *Geophys. Res. B* 89, 525-534.
- Evins, L.Z., Jensen, K.A., Ewing, R.C., 2005. Uraninite recrystallization and Pb loss in the Oklo and Bangombe natural fission reactors, Gabon. *Geochim. Cosmochim. Acta* 69, 1589-1606.
- Ewing, R.C., 1999. Nuclear waste forms for actinides. *Proc. Nat. Acad. Sci. USA* 96, 3432-3439.
- Ewing, R.C., Chakoumakos, B.C., Lumpkin, G.R., Murakami, T., Gregor, R.B., Lytle, F.W., 1988. Metamict minerals: Natural analogues for radiation damage effects in ceramic nuclear waste forms. *Nucl. Instr. Methods Phys. Res.* 32, 487-497.
- Ewing, R.C., Lutze, W., Weber, W.J., 1995. Zircon: A host-phase for the disposal of weapons plutonium. *J. Mater. Res.* 10, 243-246.
- Ewing, R.C., Meldrum, A., Wang, L.M., Weber, W.J., Corrales, L.R., 2003. Radiation effects in zircon. In: Hanchar, J.M., Hoskin, P.W.O. (Eds.), *Zircon*, Mineralogical Society of America, Washington, DC, pp. 387-425.
- Geisler, T., Ulonska, M., Schleicher, H., Pidgeon, R.T., van Bronswijk, W., 2001. Leaching and differential recrystallization of metamict zircon under experimental hydrothermal conditions. *Contrib. Mineral. Petrol.* 141, 53-65.

- Geisler, T., Pidgeon, R.T., van Bronswijk, W., Kurtz, R., 2002. Transport of uranium, thorium, and lead in metamict zircon under low-temperature hydrothermal conditions. *Chem. Geol.* 191, 141-154.
- Geisler, T., Rashwan, A.A., Rahn, M., Poller, U., Zwingmann, H., Pidgeon, R.T., Schleicher, H., 2003. Low-temperature hydrothermal alteration of natural metamict zircons from the Eastern Desert, Egypt. *Mineral. Mag.* 67, 485-508.
- Hidaka, H., Shimizu, H., Adachi, M., 2002. U-Pb geochronology and REE geochemistry of zircons from Palaeoproterozoic paragneiss clasts in the Mesozoic Kamiaso conglomerate, central Japan: evidence for an Archean provenance. *Chem. Geol.* 187, 279-293.
- Horie, K., Hidaka, H., Gauthier-Lafaye, F., 2004. U-Pb zircon geochronology of the Franceville series at Bidoudouma, Gabon. *Geochim. Cosmochim. Acta*, 68, A511.
- Mathieu, R., Zetterstrom, L., Cuney, M., Gauthier-Lafaye, F. and Hidaka, H., 2001. Alteration of monazite and zircon and lead migration as geochemical tracers of fluid paleocirculations around the Oklo-Okelobondo and Bangombe natural nuclear reaction zones (Franceville basin, Gabon). *Chem. Geol.* 171, 147-171.
- Nasdala, L., Irmer, G., Wolf, D., 1995. The degree of metamictization in zircon: a Raman spectroscopic study. *Eur. J. Miner.* 7, 471-478.
- Nasdala, L., Zhang, M., Kempe, U., Panczer, G., Gaft, M., Andrut, M., Plotze, M., 2003. Spectroscopic methods applied to zircon. In: Hanchar, J.M., Hoskin, P.W.O. (Eds.), *Zircon*, Mineralogical Society of America, Washington, DC, pp. 427-467.
- Palenik, C.S., Nasdala, L., Ewing, R.C., 2003. Radiation damage in zircon. *Am. Mineral.* 88, 770-781.
- Pidgeon, R.T., O'Neil, J.R., Silver, L.T., 1966. Uranium and lead isotopic stability in a metamict zircon under experimental hydrothermal conditions. *Science* 154,

1538-1540.

Utsunomiya, S., Palenik, C.S., Valley, J.W., Cavosie, A.J., Wilde, S.A., Ewing, R.C.,  
2004. Nanoscale occurrence of Pb in an Archean zircon. *Geochim. Cosmochim.  
Acta* 68, 4679-4686.

Zhang, M., Salje, E.K.H., Farnan, I., Graeme-Barber, I., Daniel, P., Ewing, R.C., Clark,  
A.M., Leroux, H., 2000. Metamictization of zircon: Raman spectroscopic study. *J.  
Phys.: Condens. Matter* 12, 1915 -1925.

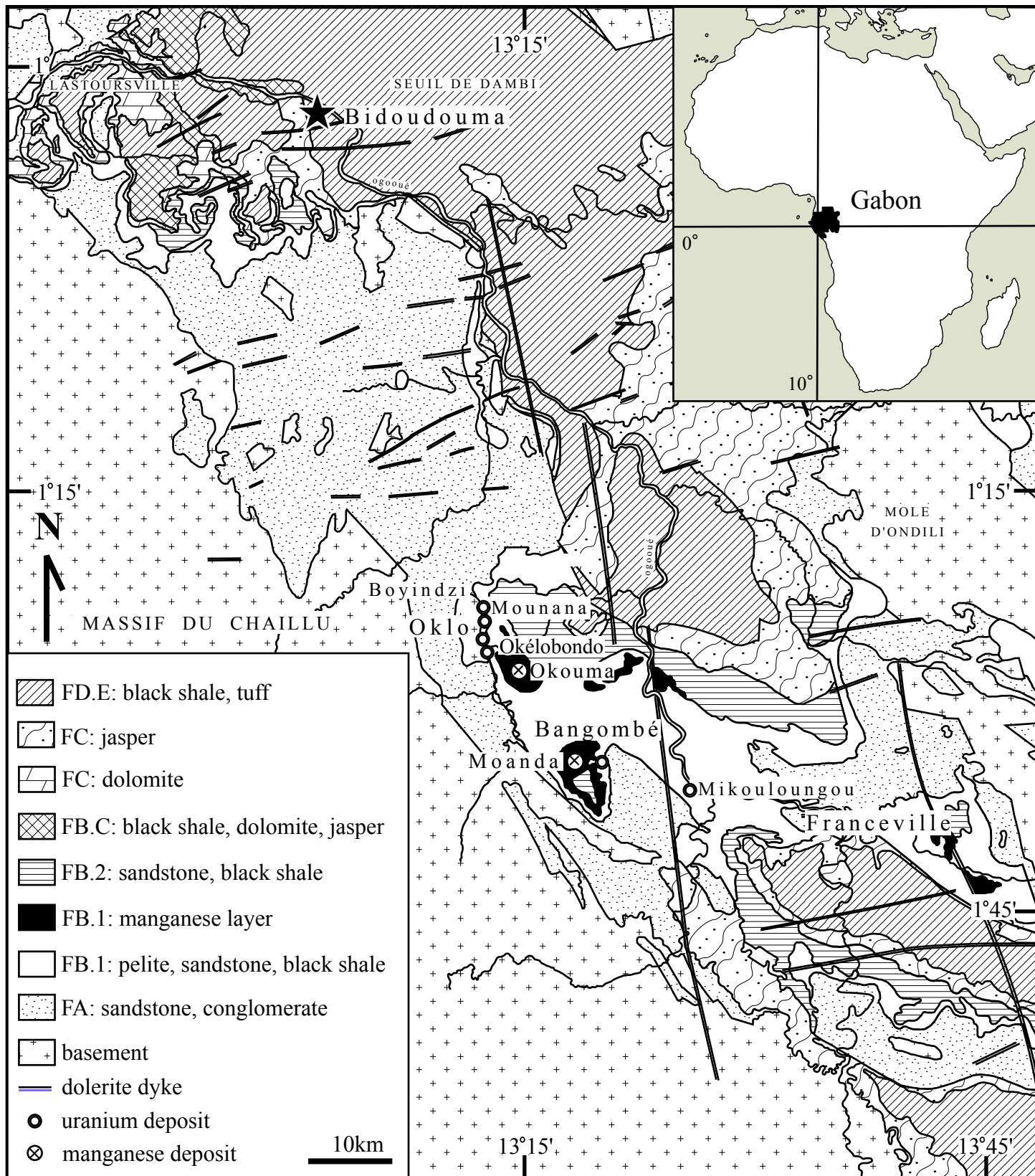
## Figure captions

Figure 1. Geological map of the Franceville region.

Figure 2. (a) Tera-Wasserburg concordia diagram of the Bidoudouma zircon. (b) Raman spectra of the discordant zircons in  $\nu(\text{SiO}_4)$  region around  $1000 \text{ cm}^{-1}$ . The  $\alpha$ -doses ( $D_\alpha$ ) given in  $10^{18}$   $\alpha$ -events per gram were calculated by using the measured U and Th concentrations and the upper intercept ages of each zircon grains. Detailed calculation method is described in Ewing et al. (2003). The gray bar is a visual guide. (c) Plot of dose vs. degree of Pb-loss and Zr-content. The Pb losses were calculated from the upper intercept age, the lower intercept age and U-Pb age of sample.

Figure 3. (a) Typical REE patterns normalized by C1 chondrite of the Bidoudouma zircons. (b) Plot of Zr content vs. Ca and Mn content. (c) Plot of Ca content vs. Fe and Al content.

Figure 4. U-content vs. the degree of Pb-loss diagram.



Horie et al. Fig.1

